Dhaka Univ. J. Sci. 69(3): 202-211, 2022 (June)
Centennial Special Issue

ISSN 1022 - 2502, E-ISSN 2408-8528
DOI: https://doi.org/10.3329/dujs.v69i3.60031

The Sensitivity of Initial Condition and Horizontal Resolution on Simulation of Tropical Cyclone Amphan over the Bay of Bengal using WRF-ARW Model

Md. Shakil Hossain[1, 2*], Md. Abdus Samad[2], Md. Saddam Hossain[3], S. M. Arif Hossen[1], Md. Asraful Islam[4], and S. M. Quamrul Hassan[5]

[1]Department of Mathematics, Khulna University of Engineering & Technology, Khulna 9203, Bangladesh
[2]Department of Applied Mathematics, University of Dhaka, Dhaka 1000, Bangladesh
[3]Department of Mathematics, Bangladesh University of Engineering and Technology, Dhaka 1000, Bangladesh
[4]Department of Meteorology, University of Dhaka, Dhaka 1000, Bangladesh
[5]Bangladesh Meteorological Department, Dhaka 1207, Bangladesh

(Received: 22 November 2021; Accepted: 14 February 2022)

Abstract

Simulation of Super Cyclonic Storm (SuCS) Amphan (2020) has been carried out as a case study to analyze the sensitivity of Initial Condition (IC) and Horizontal Resolution (HR) on the intensity, track, and landfall predictions of the Tropical Cyclones (TCs). The results suggest that the IC and HR have a significant impact on TC simulations. Diminishing the HR in simulation results in a comparatively higher severity of the system. The simulation with a reduced lead time and a comparatively smaller HR has forecasted the Minimum Central Pressure (MCP) distribution reasonably well. In comparison to the observations, the reduced lead time model run with higher resolution has forecasted the Maximum Sustained Wind Speed (MSWS) distribution precisely. According to the statistical analysis, the continual reduction of lead time in simulation with the HR of 27 km has simulated better track and landfall positions than other resolutions. Thus, the combination of reduced lead time and higher resolution in simulation may be considered for the proper track and landfall forecasting.

Keywords: Amphan, WRF, horizontal resolution, initial condition, intensity, tropical cyclone, track

I. Introduction

TCs are the deadliest environmental disasters, having a devastating impact on the way of environment, economy, and social systems. Every year, approximately 80-90 TCs form around the world, with more than half of them attains wind speeds of 65 knots or higher[1]. Among them, nearly 7% of the total yearly worldwide number of TCs form over the Bay of Bengal (BoB)[2]. The pre-monsoon (March-May) and the post-monsoon (October-December) seasons are the most frequently reported periods when the majority of the TCs form and intensify over the BoB. During these periods, the low-pressure systems that form over the regions are significantly influenced by the predominating monsoon channel over the Indian Ocean to develop into a stable cyclonic system[3].

Every year, TCs cause massive damage to people and property all around the world. TCs have resulted in the deaths of around 1.9 million people worldwide during the previous two centuries. It is also predicted that TCs may destroy the lives of 10,000 people per year[4]. According to the associated death number of casualties, the Indian subcontinent is one of the severely devasted regions of the world.As an instance, approximately 300,000 to 500,000 deaths were reported by the Great Bhola Cyclone of 1970, which crossed through the Bangladesh coast on November 12[5]. Many lives will be saved and property damage will be minimized if these cyclones can be predicted accurately in advance.

Numerous modeling and observational approaches are being studied by several researchers to develop effective TC prediction techniques. Sousounis *et al*.[6] used the WRF, RUC, MM5, and ETA models to analyze some severe precipitation cases. They concluded that the WRF model can generate more physically accurate fine-scale structures than other models. The performance of WRF-ARW model in genesis, intensity, and track forecasting of TCs is reasonably well[7, 8]. The Kain–Fritsch (KF) convection, LIN explicit microphysics schemes, Yonsei University (YSU) Planetary Boundary Layer (PBL), and NOAH land surface schemes are effective combinations for proper track and intensity forecasting[9].

Krishnamurti (1990) analyzed monsoon prediction using multiple resolutions and concluded that higher resolution models simulate more accurate precipitation[10]. It is also found that grid spacing influences the amount of precipitation predicted by the model[11]. Bhaskar Rao *et al.*[12] revealed that higher resolution results in an increased intensity but does not influence the storm's track. It is also found that the track and other cyclone parameters are strongly influenced by HRs[13]. Cacciamani *et al*.[14] studied the sensitivity of IC and HR on the numerical simulation of heavy precipitation events south of the Alps. They found that enhancing the resolution improves prediction in general. Raju *et al*.[15] concluded that the landfall timing and intensity defects diminish with the delayed ICs.

*Author for Correspondence. e-mail: shakildu192@gmail.com

As TCs are becoming more severe due to global warming, the civilization of the Indian subcontinent's low-lying coastal areas may become more challenging. It is essential to forecast TCs properly in advance to minimize casualties and property damage. The choice of horizontal grid resolution and IC are crucial for an accurate representation of the dynamic interaction of cumulus-scale and synoptic-scale circulations in numerical modeling. The sensitivity of HR in TC Amphan forecasting using the WRF model is studied in this paper. This paper is expected to have an impact on the development of the Numerical Weather Prediction (NWP) models HR standards for better TC simulation.

II. Case Study

TC Amphan was the first SuCS to cross over the BoB since the Odisha SuCS in 1999. It developed from a well-organized low-pressure system over southeast BoB and neighboring regions around 0300 UTC of 14 May. It subsequently concentrated into a Depression (D) and Deep Depression (DD) across southeast BoB in the early morning and afternoon of May 16 under favorable climatic circumstances. Moving north-northwestwards, it strengthened into Cyclonic Storm (CS) Amphan around 1200 UTC of 16 May. It further shaped into a Severe Cyclonic Storm (SCS) and Very Severe Cyclonic Storm (VSCS) over the same regions by the morning and afternoon of 17 May respectively. After forming Extremely Severe Cyclonic Storm (ESCS) by 2100 UTC of 17 May, the system developed as a SuCS approximately at 0600 UTC of 18 May. The lowest Estimated Central Pressure (ECP) and the MSWS of the system was observed as 920 hPa and 130 knots respectively between 1800 UTC of 18 May to 0000 UTC of 19 May. During 1000-1200 UTC of 20 May, the system passed the West Bengal-Bangladesh coastlines across the Sundarbans, near latitude 21.65°N/longitude 88.30°E, with MSWS of 85 knots[16]. Between D to D, the system's total duration was recorded as 138 hr.

III. Data and Methodology

The WRF model[17] version 4.3.1 has been run on a single domain at multiple resolutions 9, 18, and 27 km for 132, 108, 84, and 60 hr based on initial conditions of 0000 UTC of 16, 17, 18, and 19 May 2020 in order to analyze the effects of IC and HR on simulation of TC Amphan over the BoB. The **Table 1** presents a summary of the model configuration used in this study.

Table 1. An overview of the WRF model configuration

WRF core	ARW
Number of domains	1
Horizontal resolutions	9, 18, and 27 km
Central points of the domain	16.5°N/86.5°E for 132 hr; 18°N/86.5°E for 108 hr; 18.5°N/86.5°E for 84 hr; 19°N/86.5°E for 60 hr simulations
Grid Points (GPs)	For 132 hr simulation: 75×75×38, 112×112×38, and 225×225×38 GPs for 27, 18, and 9 km HRs respectively
	For 108 hr simulation: 70×70×38, 107×107×38, and 210×210×38 GPs for 27, 18, and 9 km HRs respectively
	For 84 hr simulation: 70×70×38, 107×107×38, and 210×210×38 GPs for 27, 18, and 9 km HRs respectively
	For 60 hr simulation: 70×70×38, 107×107×38, and 210×210×38 GPs for 27, 18, and 9 km HRs respectively
Microphysics	Kessler Scheme
PBL Parameterization	Yonsei University (YSU) Scheme
Surface layer physics	Revised MM5 Scheme
Land surface model	Unified Noah LSM
Short wave radiation	Dudhia Scheme
Long wave radiation	RRTM Scheme
Cumulus Parameterization	Kain-Fritsch (new Eta) Scheme

The Global Data Assimilation System (GDAS) accumulates observed data from the Global Telecommunications System (GTS) as well as other sources on a regular basis for a wide range of studies. The National Centers for Environmental Prediction (NCEP) prepares FNL (Final) operational global analysis and forecast data on (0.25°×0.25°) grids. Data of these datasets from 0000 UTC of 16 May to 0000 UTC of 22 May 2020 has been used in this study. To verify the impact of IC and HR, the model's outcome was compared to the observed data of India Meteorological Department (IMD)[16].

IV. Results and Discussion

The HR and IC are some of the most crucial factors that influences the intensity, landfall, and track pattern of TCs. The HR of the mesoscale atmospheric model has significantly improved due to advances in computational technology. This section analyzes the impact of HR and IC on the simulated cyclone track and intensity forecast using the WRF-ARW model.

Mean Sea Level Pressure Analysis

SuCS Amphan (2020) has been simulated as a case study to investigate the effect of several horizontal grid spacings on intensity forecasts. The WRF-ARW model has been run for 9, 18, and 27 km HR configurations using ICs on the 0000 UTC of 16, 17, 18, and 19 May 2020. The distribution of the model forecasted MCP along with the observed ECP has been presented in **Figure 1**(a-d). According to the 0000 UTC of 16 and 17 May ICs based model run, the severity of the system seems to be increased till 19 May. The observed lowest ECP of the system is 920 hPa. The simulation utilizing HR of 9 km based on 0000 UTC of 18 May has also predicted the MCP as 920 hPa which indicates about the suitability of the model. The remaining predicted MCP values are comparatively higher than the observed ECP.

Although the predicted MCPs are higher than the lowest ECP, the MCP patterns for the 132 and 108 hr simulations demonstrate relatively lower values within most of the time series. In other words, the simulated intensity is higher than the observations. On the contrary, the MCP patterns for the 84 and 60 hr simulations exhibit comparatively higher values within most of the time series, that is, the forecasted severity is lower than the observations. The reduction of HR in simulation predicts a considerably higher severity pattern of the system for 84 and 60 hr simulations. It is found that the simulation utilizing HR of 9 km depicts a relatively higher assurance to measuring the system's maximal intensity. The simulated MCP pattern for HR of 9 km demonstrates comparatively better agreement with the observations.

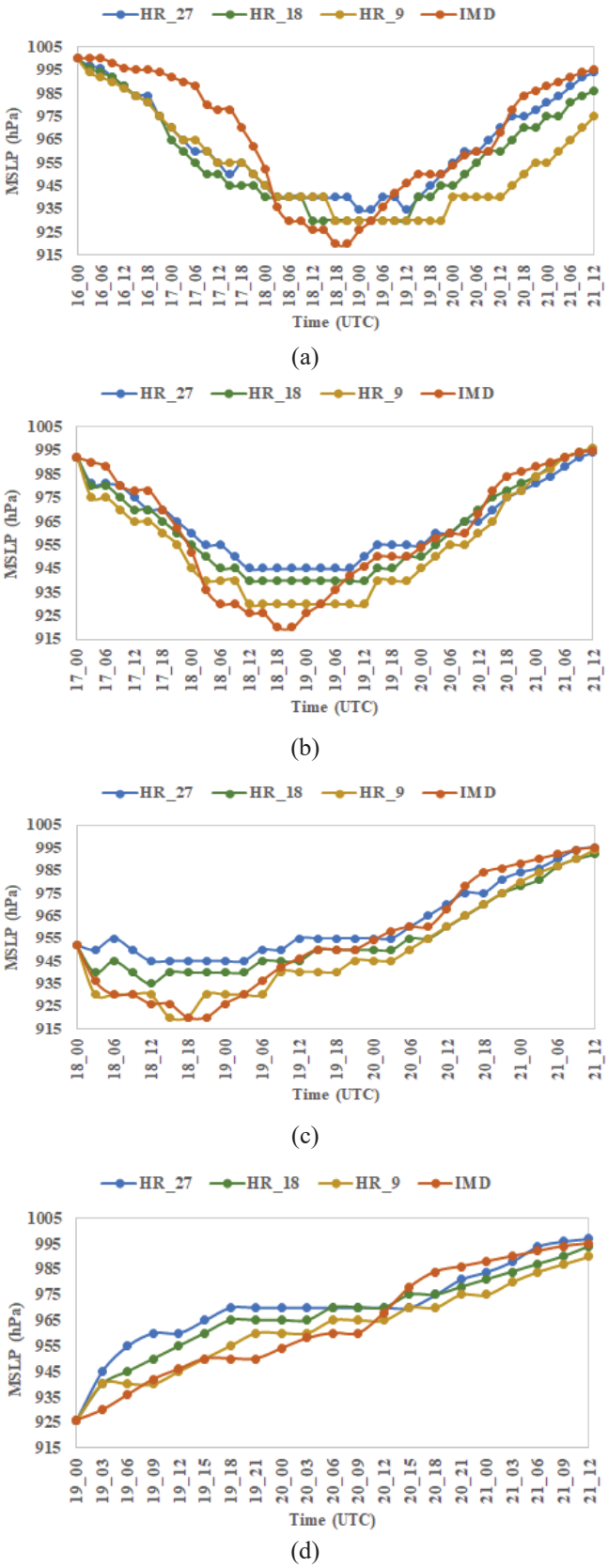

Fig. 1. Time series of simulated MCP distribution along with the ECP for 27, 18, and 9 km HRs based on 0000 UTC of (a) 16 (b) 17 (c) 18, and (d) 19 May 2020, respectively.

The forecasted peak intensity has been investigated on the basis of MCP for all simulations. The predicted MCPs are determined at around 0000, 0600, and 0000 UTC of 19 May, 2100, 1500, and 1500 UTC of 18 May, 2100, 1200, and 1500 UTC of 18 May, and 0300, 0600, and 0600 UTC of 19 May for 132, 108, 84 and 60 hr model run using 27, 18, and 9 km HRs respectively. The corresponding MCPs are 935, 930, and 930 hPa, 945, 940, and 930 hPa, 945, 930, and 920 hPa, and 945, 940, and 940 hPa respectively. It is noticed that the predicted maximum intensity timings and values in terms of the MCP varies slightly for several HRs and ICs.

The forecasted landfall timing and position has been investigated in this study. The simulated landfall times are found approximately at 2200 UTC of 20 May, 2300 UTC of 20 May, and 0200 UTC of 21 May, 1800 UTC of 20, 1300 UTC of 20, and 1100 UTC of 21 May, 1600 UTC of 20, 1600 UTC of 20, and 1500 UTC of 21 May, 1500 UTC of 20, 1700 UTC of 20, and 1700 UTC of 21 May for 132, 108, 84, and 60 hr model run with 27, 18, and 9 km HRs respectively. The corresponding landfall positions are 21.73°N/88.39°E, 21.71°N/87.97°E, and 21.62°N/87.5°E, 21.79°N/88.02°E, 21.64°N/87.57°E, and 21.75°N/87.9°E, 21.80°N/88.06°E, 21.77°N/87.79°E, and 21.75°N/87.73°E, and 21.74°N/88.91°E, 21.72°N/88.36°E, and 21.78°N/88.13°E respectively. At the time of model simulated landfall, the model simulated MCPs are 978, 970, and 960 hPa, 975, 970, and 960 hPa, 975, 965, and 965 hPa and 970, 975, and 970 hPa for 132, 108, 84, and 60 hr simulation for 27, 18, and 9 km HRs respectively. Analyzing the preceding intensity and landfall phases, it can be decided that the model generates higher intensity with the reduction of HRs.

Analysis of Wind Flow Distribution

The distribution of all simulations using several HRs has been demonstrated along with the IMD's observations in **Figure 2**(a-d). According to the predicted outcome analysis, all of the simulations MSWS changing patterns are characteristically identical. Although the behaviors of the majority of the simulations are almost identical, there are significant variations in the actual details, particularly in terms of MSWS based severity. For all HRs, it is found that the model has simulated a higher MSWS pattern than the observations. It is also observed that the model generates higher severity on the basis of MSWS with the declination of HRs. The intensity of the simulated system comparatively decreases with the enhancement of HRs. After the system's landfall, the wind speed has dropped progressively due to the surface roughness. All of the simulations overestimated the MSWS dropping pattern after the system's landfall. Above all, the simulations with higher resolution clearly demonstrate significantly better consistency with the observations.

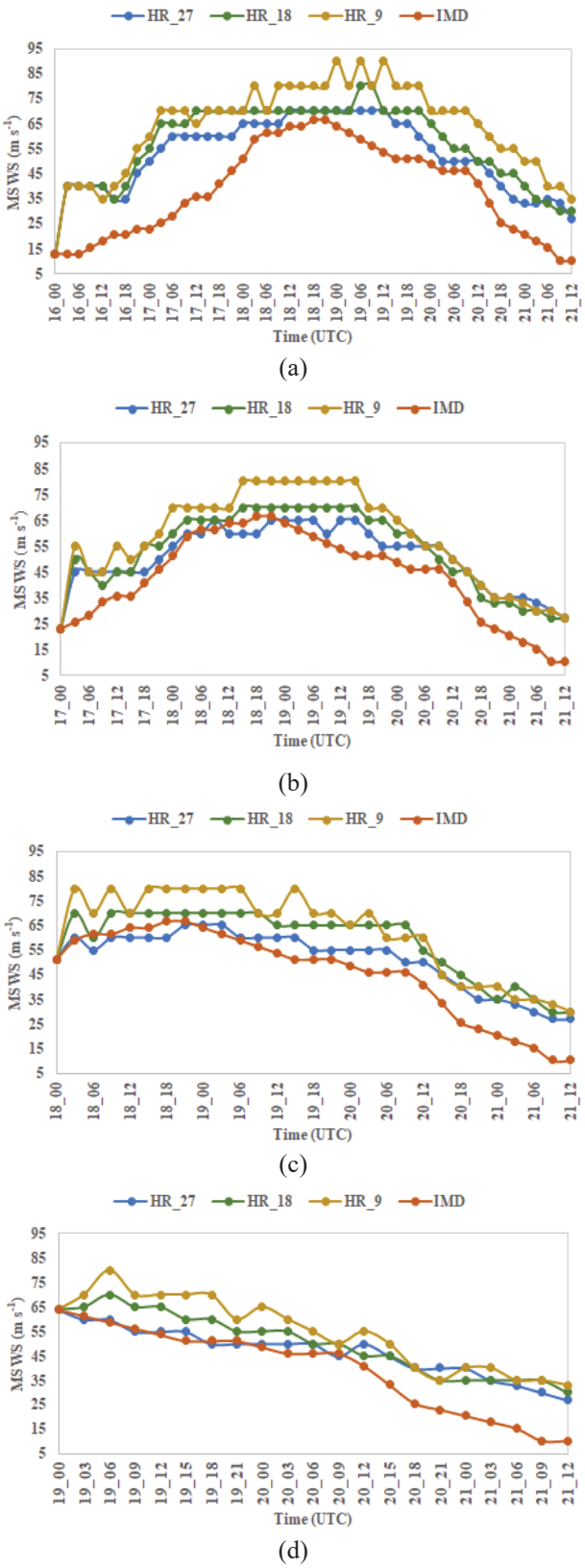

Fig. 2. Time series of simulated MSWS distribution along with the IMD's observation for 27, 18, and 9 km HRs based on 0000 UTC of (a) 16 (b) 17 (c) 18, and (d) 19 May 2020, respectively.

A well-organized convergence zone of surface wind is forecasted in all simulations, which absorbs moisture and heat from the sea surface, facilitating the development of suitable conditions for TCs and the accomplishment of their maximum strength. The observed MSWS of the system was 67 m s^{-1}. The simulated MSWS values of the cyclone are determined as approximately 70, 80, and 90 m s^{-1}, 65, 70, and 80 m s^{-1}, 65, 70, and 80 m s^{-1}, and 60, 70, and 80 m s^{-1} for 27, 18, and 9 km HRs based on 132, 108, 84, and 60 hr simulations respectively. The forecasted MSWS values of the SuCS at the time of the landfalling phase are about 35, 40, and 45 m s^{-1}, 35, 50, and 50 m s^{-1}, 45, 45, and 45 m s^{-1}, and 40, 40, and 45 m s^{-1} for 27, 18, and 9 km HRs based on 132, 108, 84, and 60 hr lead time simulations, respectively. All simulations conducted using HRs of 9 km generate MSWS values that are significantly higher than the observations. Furthermore, it is obvious that the model run by applying higher resolutions seems to have considerably better agreement with the observations, despite some errors.

Track Forecast Analysis

A proper track forecast is essential for determining the geographical area where severe damage may arise from strong winds and heavy precipitation. A precise track forecast might be quite helpful in the disaster management system. Figure **3**(a-d) depicts the track forecast of the selected cyclone for 132, 108, 84, and 60 hr model run with HRs of 27, 18, and 9 km, respectively. The position of MCP has been used to construct the track of the system. The simulated tracks are compared to the IMD's observed track to evaluate the influence of ICs and HRs.

The simulated tracks using different HRs and ICs exhibit similar features in terms of the predicted cyclone's motion and direction, despite some deviations. In comparison, the predicted track accords with the IMD results for the first 36 hr, then the track gradually deviates westward in the direction of motion for 132, 108, and 84 hr based simulations. In contrast, only the 60 hr lead time simulation with the HR of 27 km demonstrated eastward deviation. The model has also forecasted delayed movement in comparison to the system's faster speed. These factors steadily increased the error after 48 hr in simulations. All of the simulations have forecasted the corresponding regions relevant to the observed trajectory, which is a good sign of the model's reliability. With the reduction of lead time in the model run, the simulated track patterns become very close to the observed track.

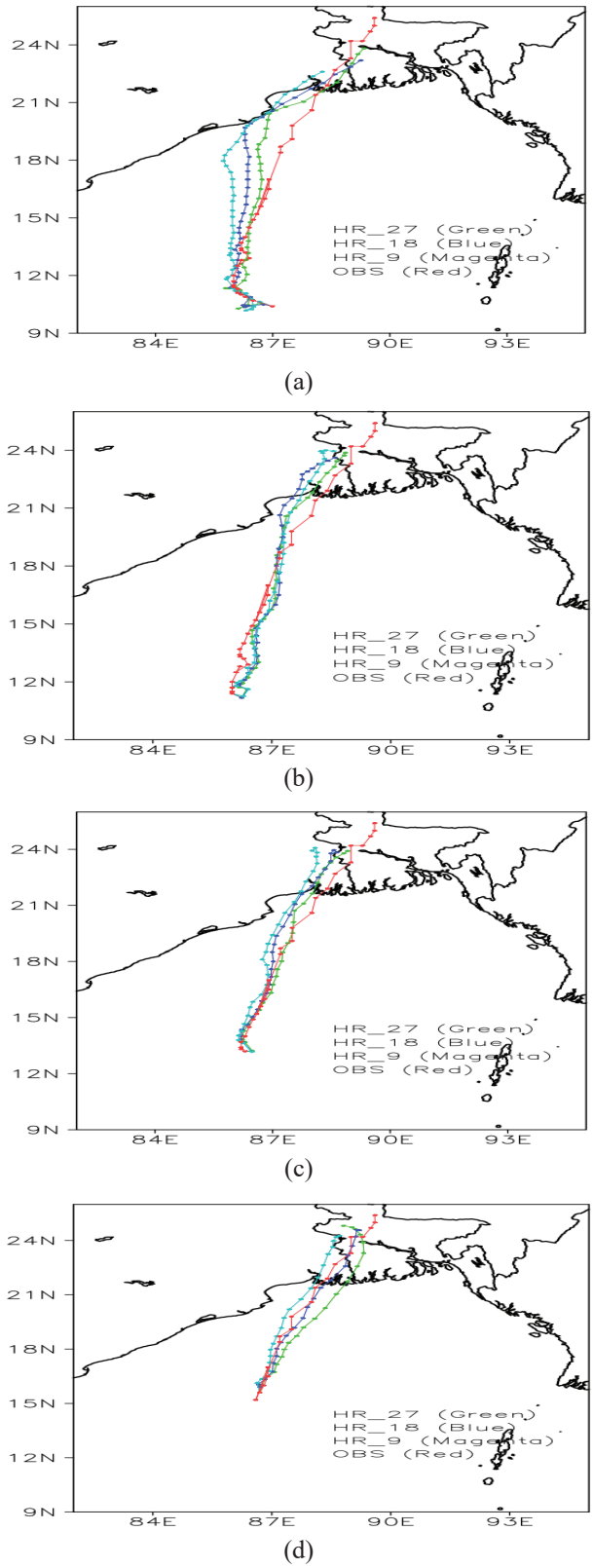

Fig. 3. Comparison of simulated track pattern along with the IMD's observed track for 27, 18, and 9 km HRs based on 0000 UTC of (a) 16 (b) 17 (c) 18, and (d) 19 May 2020, respectively.

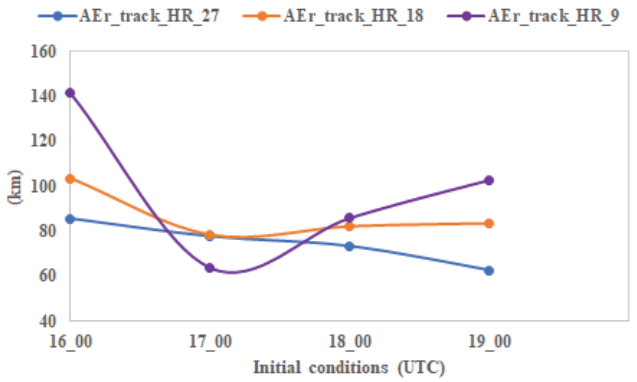

(a)

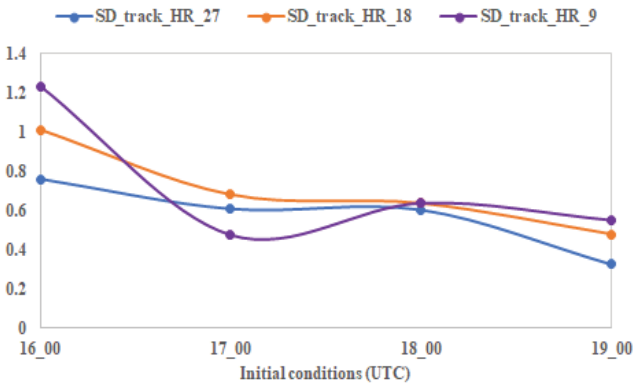

(b)

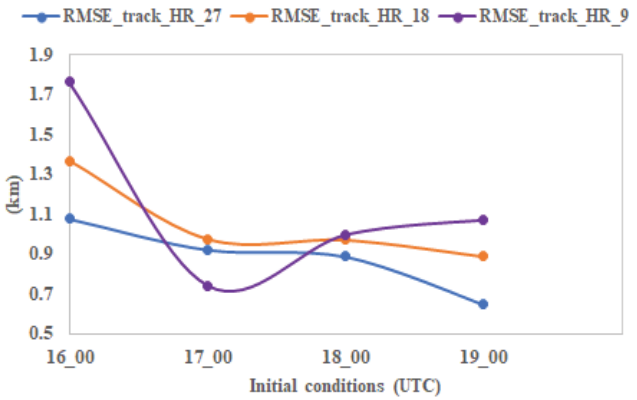

(c)

Fig. 4. Graphical presentation of computed (a) average error (b) SD, and (c) RMSE distribution of the simulated track patterns.

The impact of IC and HR on track forecasting has been assessed by analyzing the Average Error (AEr), Standard Deviation (SD), and Root Mean Square Error (RMSE) values of the simulated results. The average error, SD, and RMSE has been calculated using the following formula:

$$AEr = \frac{\sum\sqrt{(x_{obs}-x_{model})^2+(y_{obs}-y_{model})^2}}{N} \quad (1)$$

$$SD = \sqrt{\frac{\sum_{i=1}^{N}(x_i-\mu)^2}{N}} \quad (2)$$

$$RMSE = \sqrt{\frac{\sum_{i=1}^{N}(x_{obs}-x_{model})^2}{N}} \quad (3)$$

Here, μ represents average error of the simulated outcomes.

The calculated average errors are found as approximately 85.48, 103.57, and 141.3 km, 77.59, 78.47, and 63.81 km, 73.23, 82.24, and 86.02 km, and 62.50, 83.57, and 102.94 km for 132, 108, 84, and 60 hr model run with HRs of 27, 18, and 9 km respectively (Figure 4(a)). The corresponding SD are computed around 0.76, 1.01, and 1.23, 0.61, 0.68, and 0.47, 0.60, 0.64, and 0.64, and 0.33, 0.48, and 0.55 respectively (Figure 4(b)). The RMSE values are about 1.08, 1.37, and 1.76 km, 0.92, 0.97, and 0.74 km, 0.89, 0.97, and 0.99 km, and 0.65, 0.89, and1.07 km respectively (Figure 4(c)).

According to the error analysis, with the continual reduction of lead time in simulation, the HR of 27 km has simulated significantly less error and improved track positions than other resolutions. In comparison with higher resolutions of 18 and 27 km, the model simulation using finer resolution (9 km) based on 0000 UTC of 18 and 19 May has exhibited considerably higher errors. These results indicate that the model with finer resolution cannot generate the rapid movement of the system well enough. Thus, it can be decided that the simulation with higher resolutions can predict the track pattern reasonably well.

Analysis of Intensity Forecast Error

The model forecasted maximum intensity timing, values, and the corresponding forecast errors has been displayed in Table 2. The average errors, SDs, and RMSEs of the forecasted MCP and MSWS distribution for all simulations have been computed and shown in Figure 5(a-f). The model simulated MCP errors are approximately 15H, 10H, and 10H hPa, 25H, 20H, and 10H hPa, 25H, 10H, and 0 hPa, and 25H, 25H, and 20H hPa respectively for 132, 108, 84, and 60 hr simulations with the HR of 27, 18, and 9 km, respectively. The calculated SDs for MCP distributions are 7.86, 8.73, and 8.92, 7.71, 5.67, and 4.39, 8.37, 5.74, and 4.24, and 6.84, 4.04, and 4.13 respectively for 27, 18, and 9 km HR respectively (Figure 5(b)). The corresponding RMSEs are 12.32, 14.95, and 18.80 hPa, 11.34, 8.61, and 8.74 hPa, 12.29, 9.68, and 7.36 hPa, and 11.83, 8.54, and 7.35 hPa respectively (Figure 5(c)).

According to the statistical analysis, simulations with comparatively finer HR (9 km) have revealed quite good agreement with the observations compared to the simulations

with higher resolutions (18 and 27 km). Reduced lead time simulation with finer HR can ensure the converging tendency towards minimum deviation in MCP based intensity prediction. In case of MSWS, the average errors are found as 14.18, 18.45, and 25.38 m s^{-1}, 8.60, 10.09, and 15.22 m s^{-1}, 7.25, 12.69 , and 16.49 m s^{-1}, and 7.83, 10.33, and 15 m s^{-1} for 132, 108, 84, and 60 hr model run with the HRs of 27, 18, and 9 km, respectively (**Figure 5**(d)). The corresponding RMSE are computed as approximately 16.49, 20.73, and 26.69 m s^{-1}, 10.28, 11.42, and 16.33 m s^{-1}, 8.89, 14.09, and 17.36 m s^{-1}, and 10.75, 12.06, and 16.22 m s^{-1} respectively (**Figure 5**(f)). Considering these errors, it is observed that the simulations using higher HRs have captured the MSWS based intensification events well enough. It can be also deduced that the influence of HR on the SD of the predicted MSWS errors is negligible.

The RMSE values for MCP and MSWS distribution for the model run based on 0000 UTC of 19 May have increased slightly. These results indicate that the model has some deficiencies in generating the rapid deepening phase of cyclones.

Table 2. Analysis of intensity forecast error

Base Date /Time (UTC)	HR (km)	Intensity Forecast			Observed Intensity			Forecast Error		
		MCP (hPa)	MSWS (m s^{-1})	Time (UTC)	ECP (hPa)	MSWS (m s^{-1})	Time (UTC)	MCP (hPa)	MSWS (m s^{-1})	Time (hr)
	27	935	70	19/00				15H	3H	6D
16 May/0000	18	930	80	19/06				10H	13H	12D
	9	930	90	19/00				10H	23H	6D
	27	945	65	18/21				25H	2L	3D
17 May/0000	18	940	70	18/15				20H	3L	3E
	9	930	80	18/15	920	67	18 May /1800	10H	13H	3D
	27	945	65	18/21				25H	2L	3D
18 May/0000	18	930	70	18/12				10H	3H	6E
	9	920	80	18/15				0	13H	3E
	27	945	60	19/03				25H	7L	9D
19 May/0000	18	945	70	19/06				25H	3H	12D
	9	940	80	19/06				20H	13H	12D

- H, L, D, and E denote magnitudes that are higher, lower, delayed, and earlier, than the observations, respectively.

Analysis of Landfall Forecast Error

The predicted Landfall Position Error (LPE) and Landfall Time Error (LTE) has been presented in **Table 3** for all HRs and ICs based simulations. The simulated outcomes based on all HRs and ICs can be regarded as reasonably well compared to the observations. The determined maximum and minimum LPEs are approximately 89 and 10 km for 132 and 60 hr model run using 9 and 18 km HRs, respectively. The simulated highest LTE is around 15 hr delay than the actual time for the 132 hr based simulation with the HR of 9 km. The 108 hr lead time simulation, conducted with the HR of 9 km, has predicted the same/consistent time as the actual landfall timing. Considering the LPE and LTE analysis, it can be revealed that the model can predict reasonably good results despite some deviations using several ICs and HRs.

Figure 6(a-b) represents the graphical depiction of forecasted LPE and LTE of all simulations. In the case of the LTE, the forecasted results of the 108 hr based simulation using HRs of 9 and 18 km are quite well. The reduction of lead time from 132 to 108 hr has resulted in a significant decrease in LTE for both HR cases. The further diminishment of the lead time in simulation has substantially increased the LTE in both cases. These findings have raised the degree of uncertainty associated with the use of those specific combinations of ICs and HRs. On the contrary, there has been a discernible improvement in the predicted landfall timing with the continued minimization of lead times for 27 km HR.

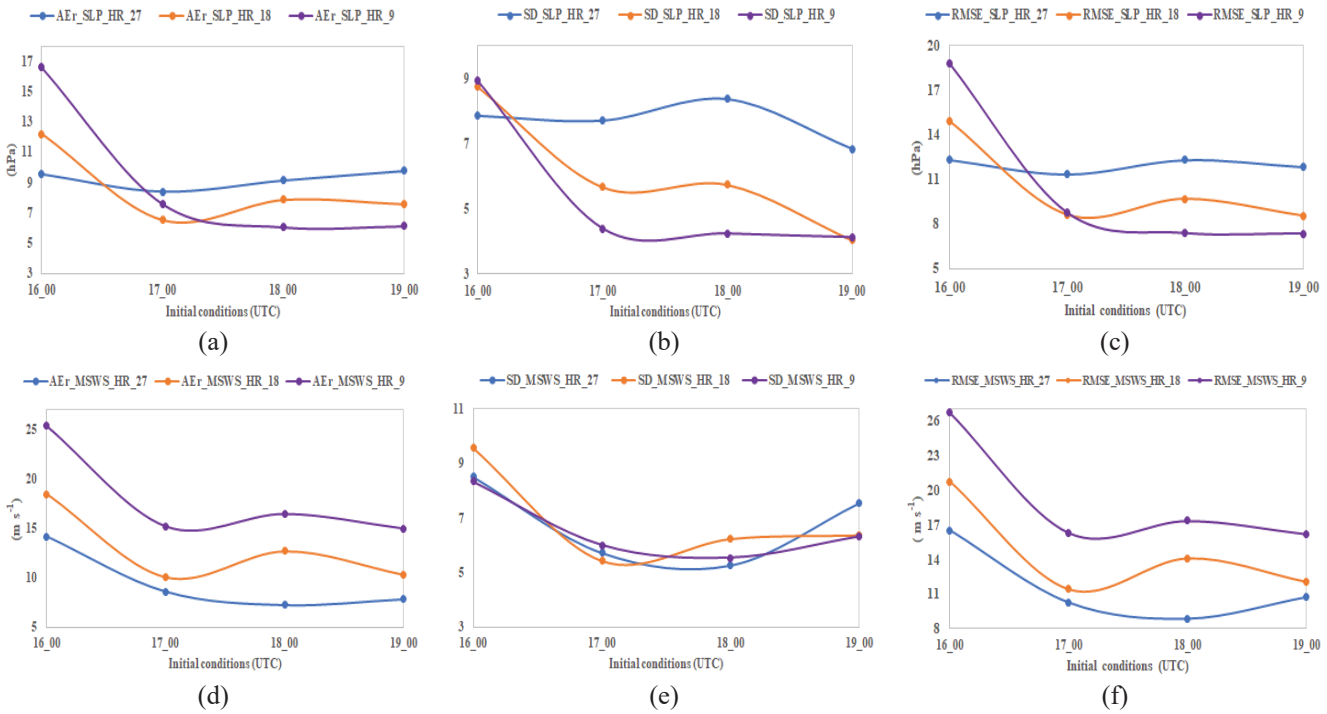

Fig. 5. Graphical presentation of computed (a) average error of MCP (b) SD of MCP (c) RMSE of MCP (d) average error of MSWS (d) SD of MSWS, and (e) RMSE of MSWS distribution of the simulated results.

Table 3. Analysis of Landfall forecast error

Base Date /Time (UTC)	HR (km)	Landfall Forecast		Observed Landfall		Forecast Error	
		Position (Lat °N/ Lon °E)	Date/Time (UTC)	Position (Lat °N/ Lon °E)	Date/ Time (UTC)	Distance (km)	Time (hour)
16 May/0000	27	21.73/88.39	20 May/2200	21.65/88.30	20 May/ 1100	13.37	11D
	18	21.71/87.97	20 May/2300			37.23	12D
	9	21.62/87.5	21 May/0200			88.86	15D
17 May/0000	27	21.79/88.02	20 May/1800			34.75	7D
	18	21.64/87.57	20 May/1300			81.04	2D
	9	21.75/87.9	20 May/1100			45.77	0
18 May/0000	27	21.8/88.06	20 May/1600			31.42	5D
	18	21.77/87.79	20 May/1600			58.16	5D
	9	21.75/87.73	20 May/1500			64.24	4D
19 May/0000	27	21.74/88.91	20 May/1500			68.44	4D
	18	21.72/88.36	20 May/1700			10.23	6D
	9	21.78/88.13	20 May/1700			23.76	6D

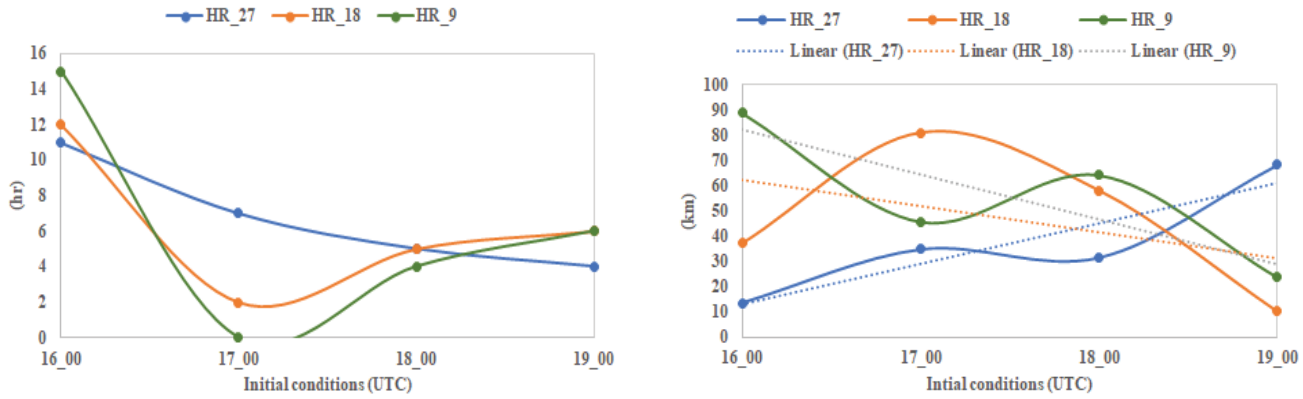

Fig. 6. Graphical presentation of computed (a) LTE and (b) LPE of the simulated landfall results.

The computed LPE from 132, 108, 84, and 60 hr simulations with HRs of 27, 18, and 9 km are 13.37, 37.23, and 88.86 km, 34.75, 81.04, and 45.77 km, 31.42, 58.16, and 64.24 km, and 68.44, 10.23, and 23.76 km, respectively (Figure **6**(b)). Except for the 60 hr based simulation, all simulations executed with the HR of 27 km have revealed a comparatively lower deviation than any other model runs. The deviations in landfall position forecast using the HR of 27 km have exhibited an upward trend as the lead time diminish. These findings indicate that the model may have some limitations in predicting proper landfalling position for a shorter lead time simulation using the HR of 27 km. The simulations with 9 and 18 km HRs have demonstrated a declining tendency in landfall location deviation as the lead time decrease. As a result, it can be said that the simulation using relatively finer resolution is more effective than higher resolutions in predicting landfall position.

V. Conclusion

One fundamental concern about existing climate models is whether the prediction of climatic events converges to a realistic depiction along with the improvement of the model's spatial and temporal resolutions. According to the above discussion, the subsequent conclusion can be drawn:

The model can represent the intensity pattern reasonably well, although it has a propensity to predict higher severity than the actual trend. The intensity pattern forecast on the basis of the MCP demonstrates significant sensitivity to ICs and HRs. It is determined that the diminishment of HRs produces a relatively higher severity of the system. In comparison to other HRs and ICs, the predicted MCP pattern using relatively lower lead time and HR demonstrates good agreement with the actual trend.

The model has some deficiencies in forecasting the MCP of the system. Except for the 0000 UTC of the 18 May based model run, all simulations demonstrate the MCP comparatively greater (relatively lower intensity) than the observations. The simulation based on 0000 UTC of 18 May has predicted the MCP to be 920 hPa, which is consistent with the real ECP. It has been found that the simulation with reduced lead time has a significant influence on the system's MCP timing and value prediction. The model run based on 0000 UTC of 19 May forecasts a considerably greater deviation in MCP timing and value prediction, which is an exceptional result compared to the rest of the simulations. The selection of the above-mentioned IC, which was 6 hr delay in the system's observed maximum intensity timing, might be the main cause of this deviation. The model's limitation in capturing the rapid intensification of the system might be another reason for this anomaly. Despite some uncertainty, it can be concluded that the combination of relatively reduced lead time and finer HR can predict a more realistic MCP based intensity distribution than other simulations.

The model produces higher intensity in terms of MSWS with the diminishment of HRs. The simulations with a comparably finer HR (9 km) have produced significantly higher intensity than the simulations with other HRs (18 and 27 km).The model run with the HR of 27 km predicted a substantially lower severity than the others.

According to the observations, the results predicted by the simulations with 27 km HR are quite reasonable. Based on the average error, SD, RMSE analysis, it can be noted that the model has some drawbacks in generating the rapid intensification events of the cyclones. Despite some deviations, it can be concluded that the relatively reduced lead times and higher HRs can be used to simulate MSWS based intensification phases more precisely.

The model can generate the system's landfalling event quite efficiently using several ICs and HRs. Despite some errors, the reduced lead time model run with the higher resolution has predicted the landfall timing reasonably well. Furthermore, it has been observed that the simulation with comparatively finer resolution is more effective than higher resolution in forecasting landfall position.

The model is capable of generating track patterns that are similar to the observations. According to the statistical analysis, the utilization of relatively higher resolutions rather than the finer resolutions in the model run reduced the deviation in the track prediction and makes the track position reasonable. The simulation with a comparatively higher resolution has captured the speedy movement of the system well enough. Thus, it can be concluded that the combination of reduced lead time and higher resolution in the simulation can be chosen for the proper track forecasting.

References

1. WMO, 2017. *Global Guide to Tropical Cyclone Forecasting (Report)*. WMO- No. 1194, Available at: https://cyclone.wmo.int/pdf/Global-Guide-to-Tropical-Cyclone-Forecasting.pdf
2. Gray, W. M., 1968. Global view of the origin of tropical disturbances and storms. *Mon. Wea. Rev.,* **96**(10), 669-700. https://doi.org/10.1175/1520-0493(1968)096%3C0669:GVOTOO%3E2.0.CO;2
3. Lee, C. S., R. Edson, and W. M. Gray, 1989. Some Large-scale characteristics associated with tropical cyclone development in the North Indian Ocean during FGGE. *Mon. Wea. Rev.,* **117**(2), 407-426. https://doi.org/10.1175/1520-0493(1989)117%3C0407:SLSCAW%3E2.0.CO;2
4. Adler, R. F., 2005. Estimating the benefit of TRMM tropical cyclone data in saving lives. American Meteorological Society, 15th Conference on Applied Climatology, Savannah, GA, 20-24 June 2005.
5. Underground, W., 2021. *Hurricane and Tropical Cyclones: The 36 Deadliest Tropical Cyclones in World History.* Available at: https://www.wunderground.com/hurricane/articles/deadliest-tropical-cyclones
6. Sousounis, P. J., T. A. Hutchinson, and S. F. Marshall, 2004. A comparison of MM5, WRF, RUC, and ETA performance for great plains heavy precipitation events during the spring of 2003. Preprints 20th Conference on Weather Analysis and Forecasting, Seattle, Amer. Meteo. Soc.
7. Hossain, M. S., M. A. Samad, M. R. Sultana, M. A. K. Malliak, and M. J. Uddin, 2021. Track and Landfall Characteristics of Very Severe Cyclonic Storm Fani over the Bay of Bengal using WRF Model. Dhaka Univ. J. Sci., **69**(2), 101-108. https://doi.org/10.3329/dujs.v69i2.56490
8. Hossain, M. S., M. A. Samad, S. M. A. Hossen, S. M. Q. Hassan, and M. A. K. Malliak, 2021. The Efficacy of the WRF-ARW Model in the Genesis and Intensity Forecast of Tropical Cyclone Fani over the Bay of Bengal. *Journal of Engineering Science,* **12**(3), 85-100. https://doi.org/10.3329/jes.v12i3.57482
9. Srinivas, C. V., D. V. Bhaskar Rao, V. Yesubabu, R. Baskaran, and B. Venkatraman, 2013. Tropical cyclone predictions over the Bay of Bengal using the high-resolution advanced research weather research and forecasting model. *Q. J. R. Meteorol. Soc.,***139**(676), 1810-1825. https://doi.org/10.1002/qj.2064
10. Krishnamurti, T. N., 1990. Monsoon prediction a different resolution with a global spectral model. *Mausam,* **41**(2), 234-240. https://doi.org/10.54302/mausam.v41i2.2546
11 . Giorgi, F., and M. R. Marinucci, 1996. An investigation of sensitivity of simulated precipitation to model resolution and its implication for climate studies. *Mon. Wea. Rev.,* **124**(1), 148-166. https://doi.org/10.1175/1520-0493(1996)124%3C0148:AIOTSO%3E2.0.CO;2
12. Bhaskar Rao, D. V., D. Hari Prasad, and D. Srinivas, 2009. Impact of horizontal resolution and the advantages of the nested domains approach in the prediction of tropical cyclone intensification and movement. *J. Geophys. Res. Atmosp.*,**114**. https://doi.org/10.1029/2008JD011623
13. Chutia, L., B. Pathak, A. Parottil, and P. K. Bhuyan, 2019. Impact of microphysics parameterizations and horizontal resolutions on simulation of "MORA" tropical cyclone over Bay of Bengal using Numerical Weather Prediction Model. Meteorol. Atmos. Phys., **131**(676), 1483-1495. https://doi.org/10.1007/s00703-018-0651-0
14. Cacciamani, C., D. Cesari, F. Grazzini, T. Paccagnella, and M. Pantone, 2000. Numerical Simulation of Intense Precipitation Events South of the Alps: Sensitivity to Initial Conditions and Horizontal Resolution. *Meteorol. Atmos. Phys.,* **72**, 147-159. https://doi.org/10.1007/s007030050012
15. Raju, P. V. S., J. Potty, and U. C. Mohanty, 2011. Sensitivity of physical parameterizations on prediction of tropical cyclone Nargis over the Bay of Bengal using WRF model. *Meteorol. Atmos. Phys.,* **113,** 125-137. https://doi.org/10.1007/s00703-011-0151-y
16. IMD, 2021. *Super Cyclonic Storm, 'AMPHAN' over Southeast Bay of Bengal (16 May - 21 May 2020): A Report.* Cyclone Warning Division, India Meteorological Department, New Delhi.
17. Skamarock, W. C., J. B. Klemp, J. Dudhia, D. O. Gill, D. M. Barker, M. G. Duda, X. Y. Huang, W. Wang, and J. G. Powers, 2008. A Description of the Advanced Research WRF Version 3; Mesoscale and Microscale Meteorology Division. *National Center for Atmospheric Research,* **113.** http://doi.org/10.5065/D68S4MVH